TIM-20-01366R2

Title: Mass Flow Rate Measurement of Pneumatically Conveyed Particles Through Acoustic Emission Detection and Electrostatic Sensing

Authors: Ge Zheng[a]

Yong Yan[b] (Corresponding author)

Yonghui Hu[a]

Wenbiao Zhang[a]

Long Yang[a]

Lanqi Li[a]

Addresses: [a] State Key Laboratory of Alternate Electrical Power System with Renewable Energy Sources

School of Control and Computer Engineering

North China Electric Power University, Beijing 102206, China

[b] School of Engineering and Digital Arts

University of Kent, Canterbury, Kent CT2 7NT, U.K.

Tel: 00441227823015

Fax: 00441227456084

Email: y.yan@kent.ac.uk

ABSTRACT

Accurate online mass flow rate measurement of pneumatically conveyed particles is desirable to convert a conventional pulverized fuel fired power station into a smart thermal power plant. This paper presents a novel method for the online measurement of the mass flow rate of pulverized fuel through acoustic emission (AE) detection and electrostatic sensing. An integrated sensing head with an AE probe and three sets of electrostatic sensor arrays is developed. The proposed method determines the particle velocity by multi-channel cross correlation of the electrostatic signals and extracts the information about mass flow rate from the AE signal arising from impacts of particles with a waveguide protruding into the flow. An analytical model that relates the energy of the AE signals, the particle velocity and the mass flow rate is established. The sensing head was mounted on vertical and horizontal sections of a 72-mm bore laboratory-scale test rig conveying fine silica particles. Experimental tests were conducted under a range of flow conditions and installation orientations to assess the performance of the developed measurement system. The results demonstrate that the sensing head should be installed in any orientation away from the elbow on the vertical section of a pipe, while for installation on a horizontal pipe the waveguide should be in the horizontal direction. The instrumentation system is capable of measuring the mass flow rate of particles in the vertical pipe with a relative error within ±6.5% regardless of the orientation of the sensing head over the mass flow rate from 7 kg/h to 25 kg/h and the particle velocity from 12 m/s to 30 m/s. Whilst on the horizontal pipe the error is within ±5.8% when the sensing head is installed with the waveguide in the horizontal direction under the same flow conditions.

Index Terms– Particle flow, pneumatic conveying, mass flow rate, acoustic emission, electrostatic sensor

I. INTRODUCTION

Pneumatic transportation of particulate solids is widely adopted in many industry sectors, such as power generation, food processing, chemical engineering, etc. The mass flow rate measurement of particles plays a vital role in improving product quality and process efficiency. In particular, coal and biomass-fired power plants can benefit from accurate measurement of fuel flow rate with improved combustion efficiency and reduced pollutant emission. Moreover, based on the mass flow rate of particles in the pipeline, optimal conveying conditions can be reached, which would reduce energy consumption and wear on equipment [1]. However, as the particle flow in fuel injection pipelines is very complex in terms of gas-solids two-phase flow nature and is in a dilute suspension, the online mass flow metering of particles is recognized as a long-standing industrial problem [2, 3].

Over the years, a diverse range of techniques and instruments have been developed and proposed to tackle this challenge. The physical sensing principles of these methods include optical [4, 5], process tomography [6, 7], microwave [8, 9], ultrasonic/acoustic [10–13] and electrostatic [14–17] techniques. Laser Doppler technique is a classic method for particle velocity and concentration measurement [4], but it is impractical to apply in coal fired power plants due to the contamination of optical components by fine dust and high maintenance cost. Process tomography is proposed for characterization of multiphase flow over the pipe cross section. Electrical capacitance tomography (ECT) is one of the typical systems for multiphase flow measurement [6]. However, due to the poor space resolution and low sensitivity, attempts to extend this technique to the particle flow in a dilute suspension have met with only limited success. Microwave techniques are based on the absorption of microwaves by particles in the pipe, but are susceptible to moisture content of particles and their deposition on the inner pipe wall [8]. Electrostatic sensing, with the

advantages of high sensitivity, structural simplicity and nonintrusiveness to the flow line, is one of the most effective methods for the measurement of particle velocity [15, 16]. Finite element modelling (FEM) of electrostatic sensors has been well studied in the past, in particular, FEM simulation of circular, probe and arc-shaped electrodes [15, 17]. There have been some studies devoted to mass flow rate measurement of particles with electrostatic sensors [14–16]. However, as the amount of charge on particles may depend on a variety of environmental and operating conditions, affecting the solids concentration measurement and hence the accuracy of mass flow rate measurement.

The instruments based on acoustic emission (AE) detection measure particle parameters by analyzing the impulsive AE signals due to impacts of particles with a plate or an AE sensor [13, 18–21]. This type of AE technique is simple, reliable and insensitive to environmental conditions such as moisture content and ambient temperature. Preliminary research was conducted by Bouchard *et al.* [18] who used an AE sensor to monitor a batch crystallization process. It was found that as particles increase in number, the peak count rate of the acoustic signal increased. Ivantsiv *et al.* [19] utilized AE techniques for mass flow rate measurement of particles in abrasive jet machining operation. The particles ejected from the nozzle direct through a mask and then impact a target plate, behind which an AE sensor is mounted. For 60 μm glass beads and 25 μm aluminum oxide powder, a significant linear correlation between the power spectral density and the mass flow rate was obtained. In the study of the influence of particle flow characteristics on the AE signal, Droubi *et al.* [20] carried out a series of erosion experiments on a slurry flow test rig. The results showed that the AE energy was proportional to the square of velocity and linear with mass concentration. Hii *et al.* [13] observed that the RMS and energy of the AE signal were positively correlated with the average kinetic energy of particles by experimental research. Wang *et al.* [21]

developed an AE-based measurement model with the calibrated reference signal for mass flow rate measurement of pneumatically conveyed particles. As the calibrated reference signal was obtained by feeding sands through a glass funnel outlet into the surface of the pipeline, the system is bulky, complex and impractical for installation in power plants. Meanwhile, the conveying air velocity was measured instead of the actual particle velocity, leading to low accuracy in mass flow rate measurement.

As the AE signal depends simultaneously on various particle flow parameters such as particle size distribution, velocity and mass flow rate of particles, it is difficult to extract only the mass flow rate of particles from the AE signal. Despite various studies over the years, there is still a lack of a simple and effective system through AE detection for online mass flow rate measurement of pneumatically conveyed particles.

This paper reports, for the first time, an integrated instrumentation system which combines the AE and electrostatic sensing techniques for the mass flow metering of pneumatically conveyed particles. The integrated sensing head consists of an AE probe and three sets of electrostatic sensor arrays each with three arc-shaped electrodes. A waveguide is introduced into the particle flow to allow the generation of an AE signal through particle impacting. Meanwhile, the electrostatic sensor arrays are incorporated to measure the particle velocity independently. The mass flow rate of particles is then derived from the particle velocity and the energy of the AE signal. This design strategy makes the best use of each sensing technique and underpins the novel flow metering instrumentation that is cost-effective and accessible to common process plants such as coal fired power stations. The concept along with preliminary results was initially reported at the 2020 IEEE International Instrumentation and Measurement Technology Conference [22]. This extended paper gives a detailed description of the fundamental principle and system design as well as practical

evaluation of the proposed mass flow metering system on both vertical and horizontal pipelines in different orientations.

II. METHODOLOGY

A. General Principle

The sensing arrangement and measurement strategy of the proposed mass flow metering system are shown in Fig. 1 and Fig. 2, respectively. AE is the class of phenomena whereby transient elastic waves in a solid object are generated due to the rapid release of energy from a localized source. For mass flow metering of particles in a pneumatic conveying pipeline, a waveguide is inserted into the flow as an impact target for the particles (Fig. 1). The impacts of the moving particles on the waveguide generate a series of transient elastic waves at the impact points and then the waves propagate along the waveguide. As the attenuation coefficient of the waves is only a few decibels per meter, the influence of different collision sites on the acquired AE signal can be negligible for a waveguide with small impact area. On the end of the waveguide, an AE sensor is attached to convert the elastic stress wave into electrical signal. The characteristics of the acquired AE signals are dependent on various particle flow parameters. For the mass flow rate metering, it is necessary to decouple the effect of the particle velocity on the AE signal. The electrostatic sensing technique is a simple but effective approach to particle velocity measurement [15, 16]. Particles in pneumatic conveying pipelines are charged due to collision of the particles with the pipe wall, impact between the particles, and friction between the particles and the air stream. Due to the electrostatic phenomenon, a certain amount of induced charge is generated on an electrode surface as the charged particles pass over the electrode. With the electrostatic signals obtained from electrostatic sensor arrays (Fig. 1), the particle velocity can be determined through multi-channel correlation

(Section II.B). With the known particle velocity, the mass flow rate of particles is eventually obtained by using the analytical model (Section II.C).

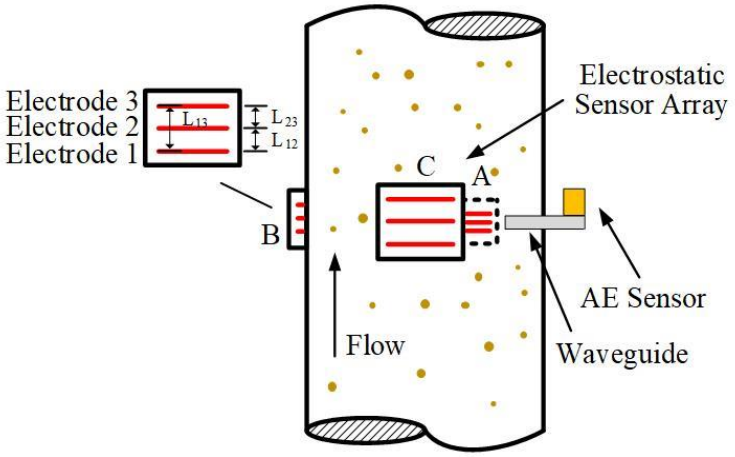

Fig. 1. Schematic illustration of the sensing arrangement (not to scale).

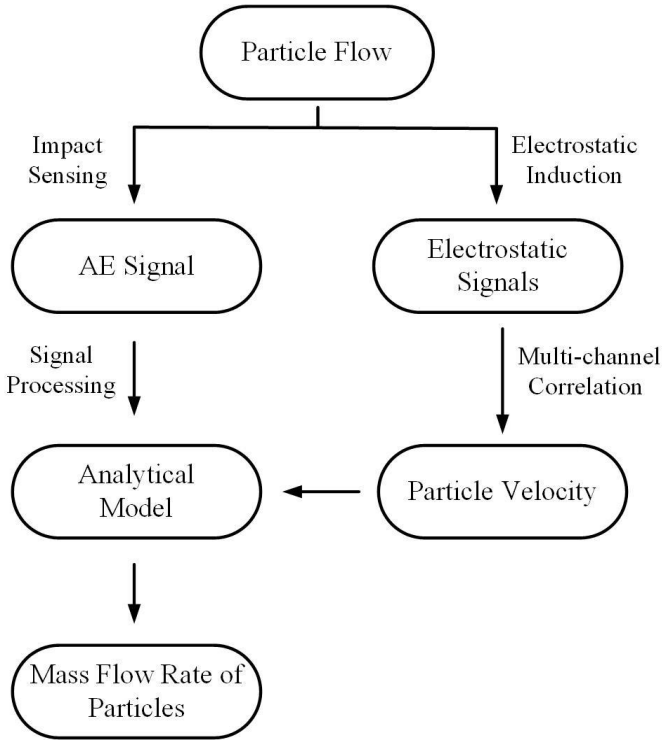

Fig. 2. Measurement strategy of the mass flow metering system.

B.Measurement of Particle Velocity

Each electrostatic sensor array contains three arc-shaped electrodes, namely electrodes 1, 2 and 3, which are distributed from upstream to downstream with an equal spacing between them (Fig. 1). Every pair of the electrodes (electrodes *i* and *j*) are used to measure the particle velocity through cross-correlation velocimetry [16]

$$v_{ij} = \frac{L_{ij}}{\tau_{ij}} \tag{1}$$

where i, j = 1, 2, or 3, L_{ij} is the axial distance between electrodes i and j, τ_{ij} is the transit time determined by cross-correlating the signals from the upstream and downstream electrodes. The transit time τ_{ij} is obtained by locating the dominant peak of the correlation function, which is defined as:

$$R_{ij}(t) = \frac{\gamma_{ij}(t)}{\sigma_i \sigma_j} \tag{2}$$

where $\gamma_{ij}(t)$ is the cross covariance between the signals from electrodes i and j, and σ_i and σ_j are the variances of the two signals, respectively. The fused average particle velocity from each sensor array, i.e. v_A, v_B and v_C, is determined from three individual velocities [16]

$$v_k = \frac{r_{12}v_{12} + r_{23}v_{23} + r_{13}v_{13}}{r_{12} + r_{23} + r_{13}} \tag{3}$$

where k is A, B or C and r_{12}, r_{23} and r_{13} are the correlation coefficients corresponding to the amplitudes of the dominant peaks of $R_{12}(t)$, $R_{23}(t)$ and $R_{13}(t)$ in eq. (2), respectively. The particle velocity (v) used in the AE signal analysis is derived by fusing the average velocities from the sensor arrays A and C (Fig. 1). Meanwhile, the mean particle velocity across the entire pipe cross section is the arithmetic mean of the three individual velocities, v_A, v_B and v_C. The sensing system

is designed for installations on industrial pneumatic conveying processes. The conveying air velocity is set to at least 7 m/s to enable particles to move forward in the pipe. A velocity below or around this value can easily lead to pipeline blockage which would affect the smooth transportation of bulk solids material or even safe operation of the industrial process. According to previous experimental results obtained from electrostatic sensors on power plants, the particle velocity is around 20 m/s [15, 16].

C. Mass Flow Rate Measurement of Particles

For pneumatically conveyed particles, the energy is mainly stored in the kinetic energy of the particles and released by collision or sliding friction. For the dispersed particles that collide normally with a plate (AE waveguide), the energy dissipation E_{loss} is given by [23, 24]

$$E_{loss} = \frac{1}{2} nm(1-k^2)v^2 \tag{4}$$

where n is the number of particle impact events per second, m is the average mass of particles, k is the coefficient of restitution, and v is the particle velocity. It is generally agreed that part of the energy dissipated as elastic waves in the form of Rayleigh waves, compression waves and shear waves [25, 26]. The energy of the AE signal (E) is regarded as being proportional to dissipated energy (E_{loss}) [27], i.e.

$$E = k_t E_{loss} \tag{5}$$

where k_t is a proportional constant depending upon a range of factors including energy conversion rate, wave propagation process, signal conditioning circuit, response characteristics of the AE sensor, etc. The energy of the AE signal (E) over a period from t_1 to t_2 can be calculated as:

$$E = \int_{t_1}^{t_2} x^2(t)dt \tag{6}$$

where $x(t)$ is the signal amplitude at time t. For the AE probe with a waveguide protruding into the flow, the mass flow rate of particles (q_m) in the pipe is given by:

$$q_m = k_c nm \tag{7}$$

where k_c depends on the blocking area of the waveguide with reference to the cross section of the pipe. Substituting eq. (7) into eq. (4) yields:

$$E = k_m q_m v^2 \tag{8}$$

where v is the mean particle velocity from the electrostatic sensor arrays and k_m is regarded as a meter factor, which can be determined through calibration.

D. System Design

Fig. 3 is the sensing head for mass flow rate measurement. As can be seen, the sensing head is composed of an AE probe and three sets of electrostatic sensor arrays each with three arc-shaped electrodes. A waveguide protrudes into the particle flow to generate and transmit AE signal due to the impact of low concentration particles. The waveguide, penetrating through the wall of the pipe, is made of zirconia ceramics, a wear-resistant material, in order to prolong the life span of the waveguide and hence avoid frequent replacement and re-calibration of the sensing system. Meanwhile, if the waveguide is heavily worn due to long-term operation, it should be readily replaced and re-calibrated to ensure cost-effective maintenance. The flat surface of the waveguide faces the direction of the flow, allowing a small fraction of the particles to collide with the surface of the waveguide perpendicularly. The protruding length of the waveguide within the pipe cross section is adjustable. After certain experimental trials and with reference to the original design, the protruding length was set to 7 mm in this study in view of the trade-off between high signal-to-noise ratio and few overlapping impacts. The resulting blockage of the waveguide is 1.7% of the

pipe cross-sectional area. Since pulverized fuel flow is very dilute (volumetric concentration is less than 0.1%) [16] and the blockage area is so small, simultaneous impact of multi particles is seldom. An AE sensor that converts the elastic stress waves into electrical signals is attached to the outer end of the waveguide with high-vacuum grease. The operating bandwidth of the AE sensor (RS-2A, Softland) is 50~400 kHz. With rubber bushings embracing the middle section of the waveguide, the AE waveguide can avoid the interfering vibrations of the pipe section. In comparison with mounting the AE sensor on the outer surface of a vessel or a pipe [28, 29], this design achieves higher sensitivity to particle flow and avoids background noise from the continuous vibration of the fuel conveying pipe. As shown in Fig. 1, three sets of electrostatic electrodes are uniformly embedded in the pipe wall, each having three identical arc-shaped electrodes with an axial width of 5 mm. The centre-to-centre spacing between the adjacent electrode pair in the flow direction is 20 mm. Every electrode is insulated from particle flow through a wear-resistant insulation layer. The electrode of this design only detects charged particles through electrostatic induction. In comparison with the circular electrodes as used in previous studies [30, 31], the arc-shaped electrode arrays measure the velocity in the local area close to the electrode, rather than the averaged velocity over the cross section. The designed electrode arrays not only have a high spatial resolution but also improve the reliability of the system through redundant configuration.

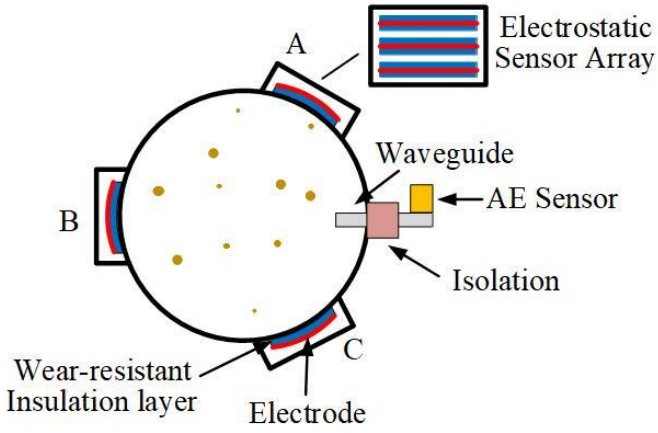

(a)

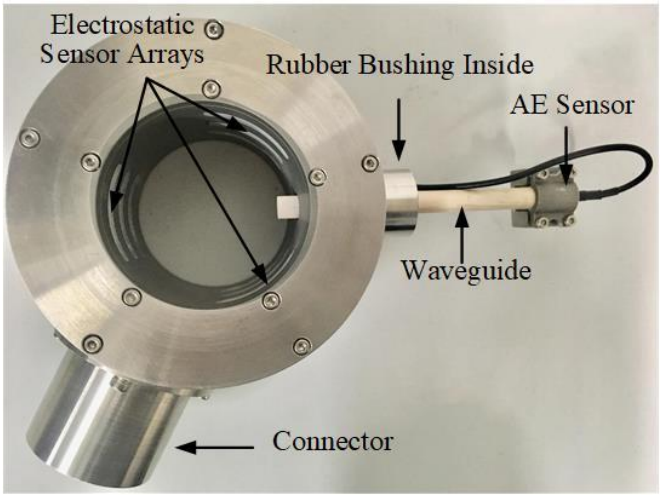

(b)

Fig. 3. Design of the sensing head. (a) Schematic diagram. (b) Photo of prototype sensing head.

Fig. 4 represents a simplified block diagram of the key elements in the measurement system. A high-speed multi-channel signal conditioning unit, constructed with high-speed operational amplifiers, is used for the filtering and amplification of the ten signals from the sensing head. The AE signal is amplified with a voltage gain of 35 dB and filtered through a band-pass filter with a frequency range of 1 kHz – 1 MHz. The signal-to-noise ratio of the AE signal conditioning unit is 40 dB. The minute current signal from each electrostatic sensor is converted into a voltage form through an I/V converter and is then amplified through a voltage amplifier with a voltage gain of 50 dB and a low-pass filter with a cut-off frequency of 2 kHz. The signal conditioning channel for each electrostatic sensor has a signal-to-noise ratio of 20 dB. The AE signal and nine electrostatic

signals are then digitized using a data acquisition device and processed on a host computer. The particle velocity and hence the mass flow rate of particles are determined by the signals.

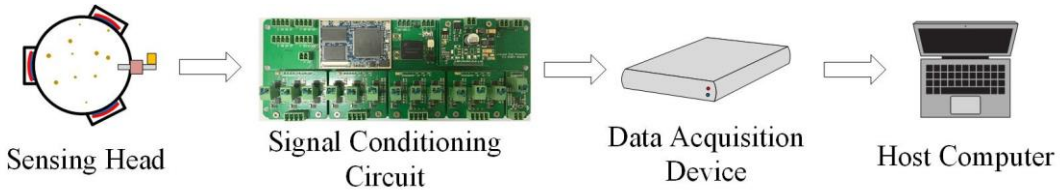

Fig. 4. Hardware block diagram of the measurement system.

III. Experimental Results and Discussion

A. Experimental conditions

To evaluate the performance of the prototype measurement system, a series of experiments were carried out on a 72-mm bore particle flow rig, as illustrated in Fig. 5. An industrial suction system is connected to the pipeline to provide a stable air flow. By regulating the power of the suction system, different particle velocities are created. A screw feeder with an embedded electronic control system is applied to keep the mass flow rate of particles at a desired value.

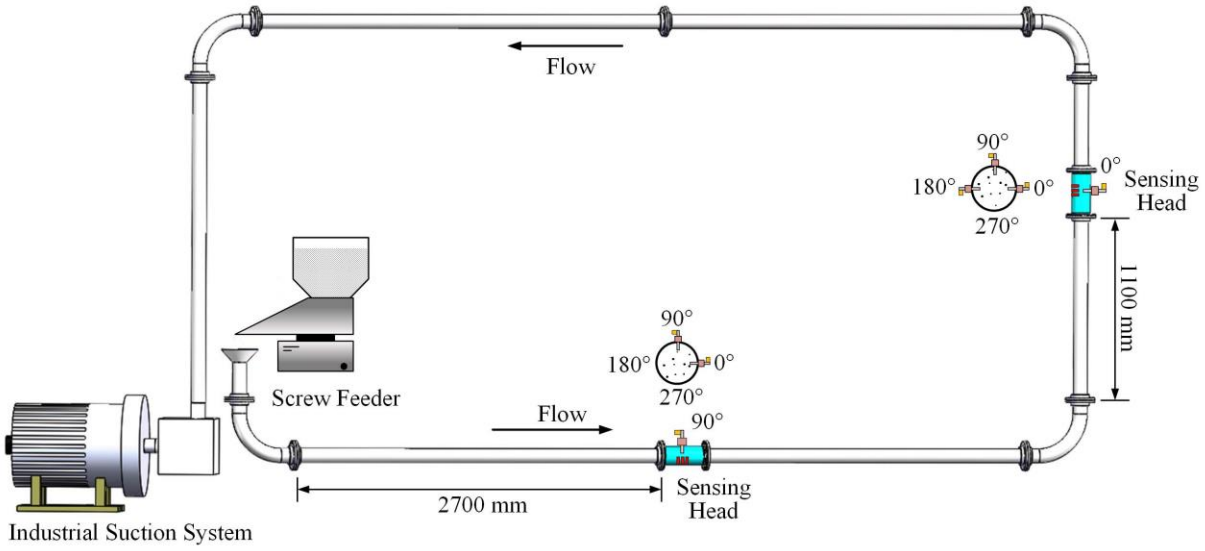

Fig. 5. Layout of the particle flow rig.

Silica sands ranging from 61 to 395 μm (measured from a laser particle size analyzer, OMEC

LS-POP9) were used as test particles in the experiments. The bulk density of the test material is 1.45 g/cm^3. The ambient temperature and relative humidity during the test period were 24.1 °C and 52%, respectively. Experimental tests over a range of conditions were conducted at each location in each orientation. A total of 7x7 test conditions were created by varying the mass flow rate of solids (7 kg/h to 25 kg/h with an increment of 3 kg/h) and particle velocity (12 m/s to 30 m/s with an interval of 3 m/s). The mass flow rate of solids was varied by regulating the particle discharge rate of the screw feeder, with a deviation of around ±0.2 kg/h from the set value. By cross-correlating the signals from the electrostatic electrodes, the particle velocity was determined and displayed on the host computer screen in real time. When the time-averaged velocity differed from the desired value by less than ±0.5 m/s, the signals were recorded for 8 seconds.

The sensing head was installed on the rig at locations where the particles are less affected by the flow turbulence in the upstream, such as away from the upstream elbow. On the vertical pipe, the distance between the sensing head and the upstream elbow is about 15D (D=72 mm), while on the horizontal pipe, the installation location is nearly 38D away from the upstream elbow. In order to quantify the effect of installation position on the measurement results, a series of experiments were undertaken with the sensing head in different orientations on the vertical and horizontal sections of the pipe, respectively (Fig. 5). According to the position of the waveguide relative to the cross-section of the pipe, experiments with the sensing head installed in three orientations on the vertical section of the pipe were carried out. Among them, 0° means that the waveguide is on the outer side of the pipe, and 180° means that the waveguide is on the inner side of the pipe. As the orientations of 90° and 270° are symmetrical in the relative position of the pipe, and the two orientations are the same relative to the elbow, the particle flow conditions in these two orientations, as confirmed by experimental observations, are basically the same. So the experiments with the sensing head

installed in the orientation of 0°, 90° and 180° on the vertical section of the pipe were conducted. For the horizontal section of the pipe shown in Fig. 5, 0° means that the waveguide is in the horizontal direction, and 90° means that the waveguide is in the vertical direction. Since particles can accumulate at the bottom of the pipe (270° orientation) due to gravity, so it is not advisable to place the waveguide vertically upwards to avoid potential pipe blockage. Since the 180° orientation is a mirror image of the 0° orientation about the pipe axis, the flow conditions in the two orientations are very similar. Therefore, the experiments were undertaken on the horizontal section where the waveguide was installed in the 0° and 90° orientations, respectively.

B. Results of model validation

Fig. 6 plots the typical raw AE signals collected when the mass flow rate was set to 7 kg/h, 16 kg/h and 25 kg/h, respectively. The particle velocity was held constant at 18.0 m/s. The energy of the AE signal in Fig. 6(a)-(c) is calculated as 696 V^2, 1897 V^2 and 2666 V^2, respectively. It is apparent that the increase in mass flow rate of particles leads to a substantial increase in the AE energy. Typical signals and their resulting correlation functions from electrostatic sensor array A are plotted in Fig. 7. It is evident that the signals from the three electrodes have similar patterns and there is a time delay among them due to the axial spacing between the electrodes. For this set of waveforms, the transit times between them are found to be τ_{12} = 1.00 ms (electrodes 1&2), τ_{23} = 0.95 ms (electrodes 2&3) and τ_{13} = 1.84 ms (electrodes 1&3), respectively, and the resulting individual particle velocities are v_{12} = 20.20 m/s, v_{23} = 21.05 m/s and v_{13} = 21.74 m/s, respectively. The correlation coefficients of the individual particle velocities are r_{12} = 0.72, r_{23} = 0.69 and r_{13} = 0.64, respectively. The fused average particle velocity from eq. (3) is thus v_A = 20.90 m/s. It is not surprising that τ_{12} differs slightly from τ_{23} and also τ_{13} is not exactly twice τ_{12} or τ_{23} (Fig. 7) and,

subsequently, the slight differences are in the measured individual particle velocities. There are several contributing factors for such differences, including fluctuations in the particle velocity profile across the pipe cross section, mechanical tolerance in the machining of the electrodes and insulators and the construction of the sensing head, and mismatches between the three channel signal conditioning electronics. The final average velocity from the three individual velocities through data fusion gives a more reliable and repeatable velocity measurement result.

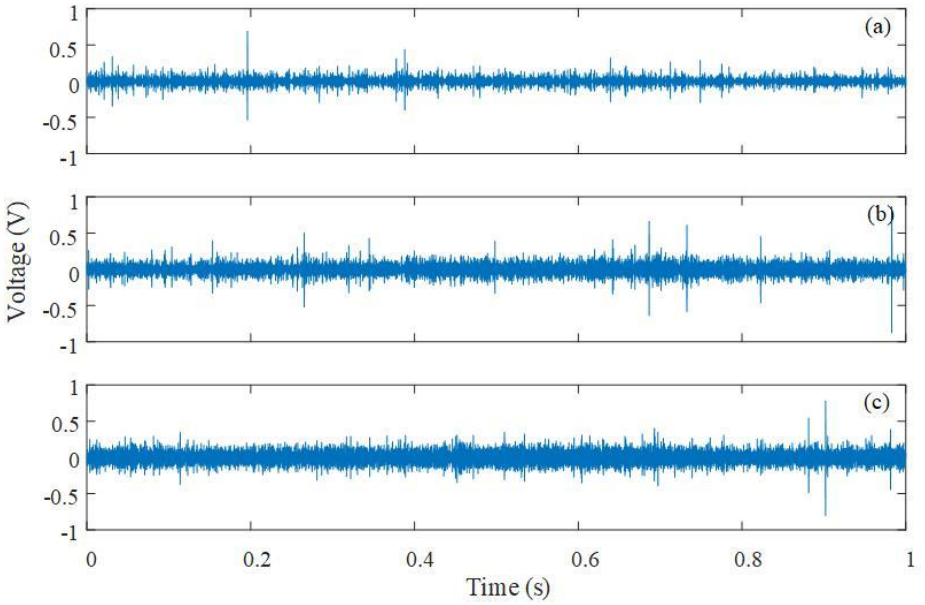

Fig. 6. Typical AE signals at different mass flow rates for a fixed particle velocity of 18 m/s. (a) 7 kg/h (b) 16 kg/h (c) 25 kg/h.

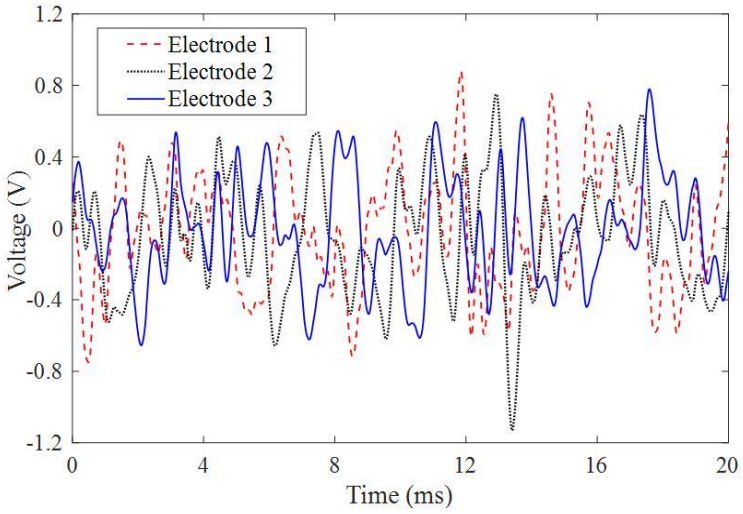

(a)

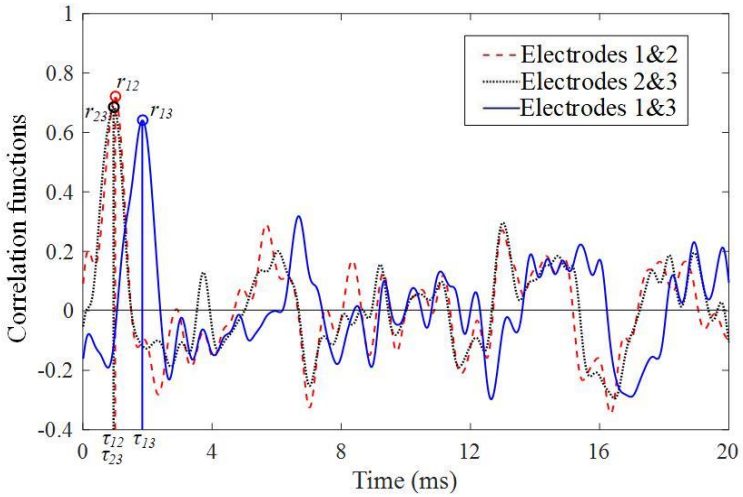

(b)

Fig. 7. Typical signals from electrostatic sensor array A and corresponding correlation functions. (a) Signal waveforms. (b) Cross-correlation functions.

For a fixed mass flow rate, the relationship between the particle velocity and the measured AE energy under all test conditions is plotted in Fig. 8. Each data point is an average of eight AE signal energies and an average of eight particle velocities over 1 second duration with the error bars representing the standard deviation of the eight values in each case. Table I lists the best fitting coefficients for all of the measurements along with the corresponding R^2 values, which describe the closeness between the measurement data and the curve fitting results. The AE energy is indeed proportional to the square of the particle velocity with R^2 values all greater than 0.99, which is in agreement with eq. (8). Fig. 9 depicts the relationship between the mass flow rate and the AE energy for a given particle velocity. Table II summarizes the quantified linear relationship between the AE energy and the mass flow rate of particles and the corresponding R^2 values. As expected, the AE energy increases linearly with the mass flow rate of particles, which is again consistent with eq. (8). In summary, the relationship between the AE energy, particle velocity and mass flow rate described in eq. (8) is verified through experimental tests.

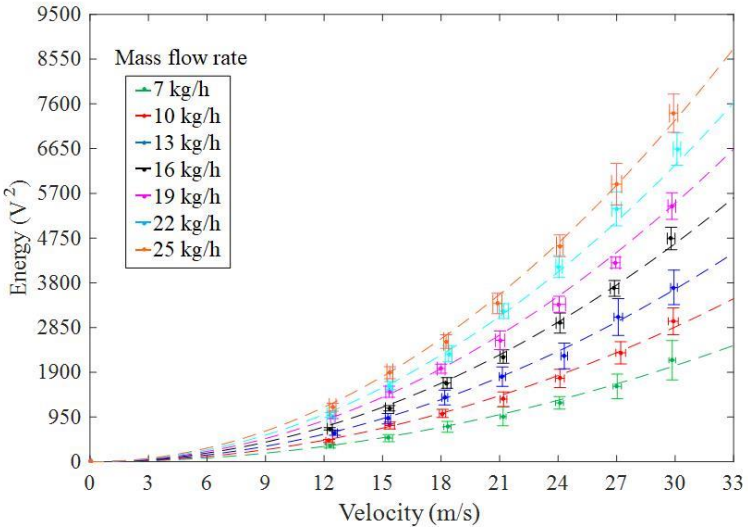

Fig. 8. Relationship between the particle velocity and the AE energy for different mass flow rates of particles.

TABLE I.

CURVE FITTING RESULTS OF AE ENERGY AND PARTICLE VELOCITY.

Mass flow rate (kg/h)	Curve fitting result	R^2
7	$E=2.27v^2$	0.9943
10	$E=3.18v^2$	0.9965
13	$E=4.07v^2$	0.9926
16	$E=5.24v^2$	0.9977
19	$E=5.96v^2$	0.9949
22	$E=7.39v^2$	0.9978
25	$E=8.06v^2$	0.9914

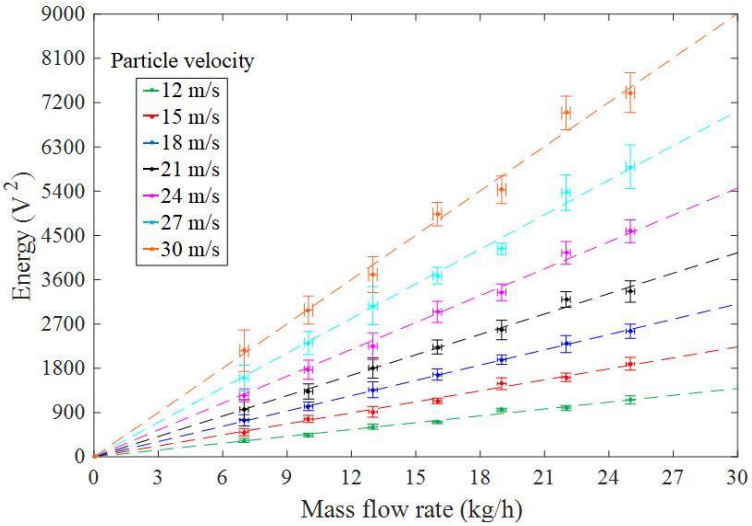

Fig. 9. Relationship between the mass flow rate and the AE energy for different particle velocities.

TABLE II.

CURVE FITTING RESULTS OF AE ENERGY AND MASS FLOW RATE.

Particle velocity (m/s)	Curve fitting result	R^2
12	$E=46.37q_m$	0.9922
15	$E=74.57q_m$	0.9950
18	$E=103.65q_m$	0.9995
21	$E=138.31q_m$	0.9957
24	$E=182.08q_m$	0.9968
27	$E=234.37q_m$	0.9961
30	$E=300.37q_m$	0.9933

C. Results of mass flow rate measurement

From the 49 datasets collected from the experimental tests under each installation orientation, 39 datasets are randomly selected for fitting a curve surface governed by eq. (8), while the remaining 10 datasets are reserved for testing the performance of the analytical model.

Figs. 10, 11 and 12 show the measurement results from the experiments in which the sensing head was installed in the three orientations (0°, 90° and 180°) on the vertical section of the pipe, respectively. The best fits of the data are also plotted together with the representing equation and R^2 value. As can be seen, for the experimental data with the sensing head installed in the 180° orientation, the coefficient K_m through curve fitting is the largest, that is, under the same test conditions, the AE energy obtained is the smallest amongst the three installation orientations. This difference is attributed to the lower particle concentration near the medial inner wall (180°) due to the influence of the centrifugal force generated when particles passed through the elbow in the upstream (Fig. 5), despite the installation location is 15D away from the elbow. In the three installation orientations on the vertical section of the pipe, the fitted curves are consistent with the measured data with high R^2 values all above 0.99, and the measured mass flow rates are close to the references with a relative error all within $\pm 6.5\%$. Therefore, on the vertical section of a pipe, the sensing head can be installed in any orientation away from the elbow.

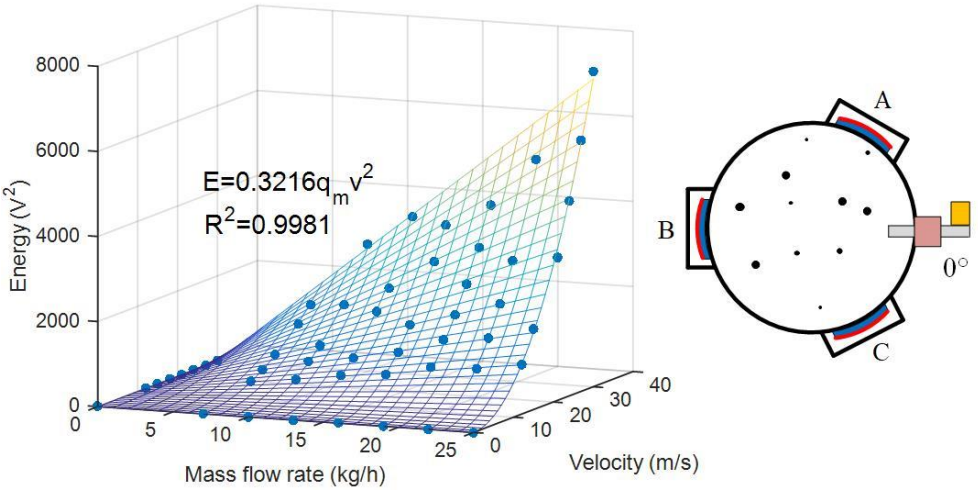

(a)

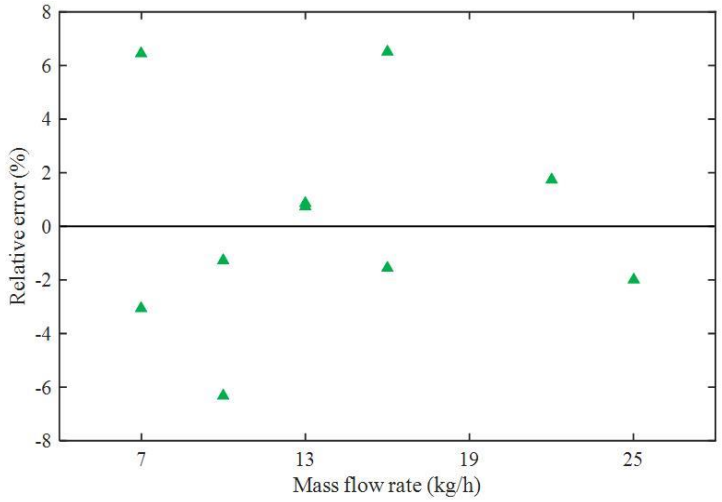

(b)

Fig. 10. Measurement results for the 0° orientation on vertical section of the pipe. (a) AE energy versus the mass flow rate and the particle velocity. (b) Relative error of the measured mass flow rate.

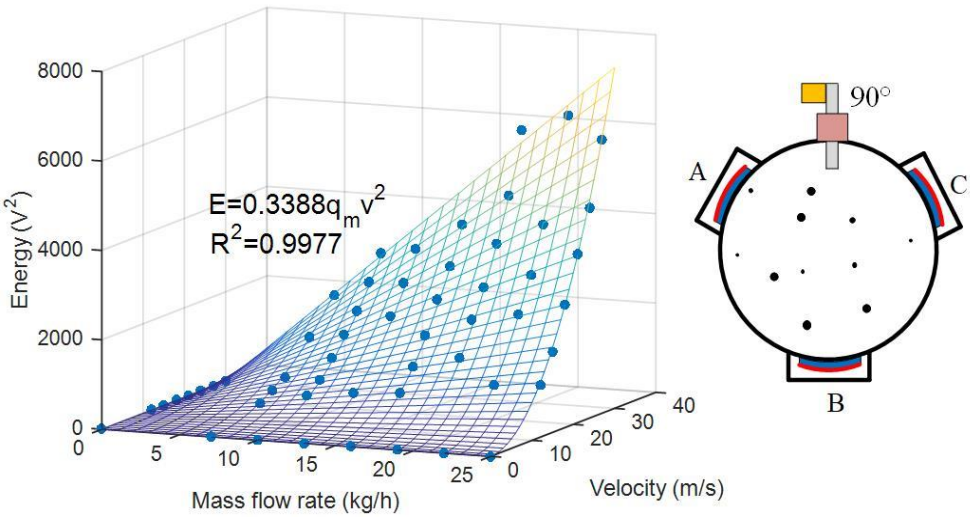

(a)

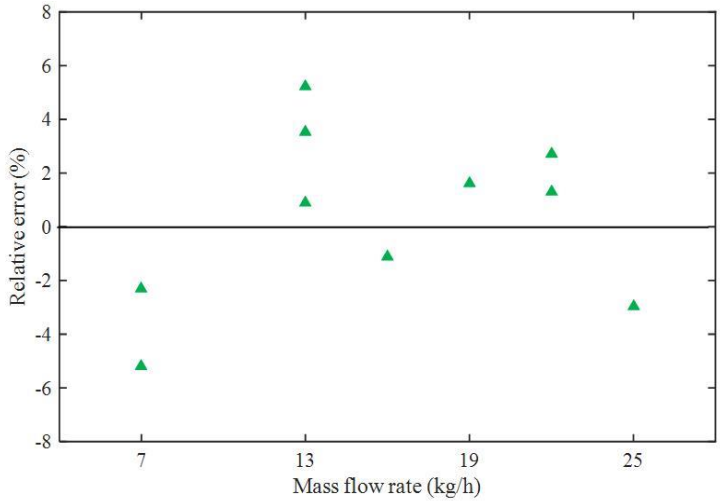

(b)

Fig. 11. Measurement results for the 90° orientation on vertical section of the pipe. (a) AE energy versus the mass flow rate and the particle velocity. (b) Relative error of the measured mass flow rate.

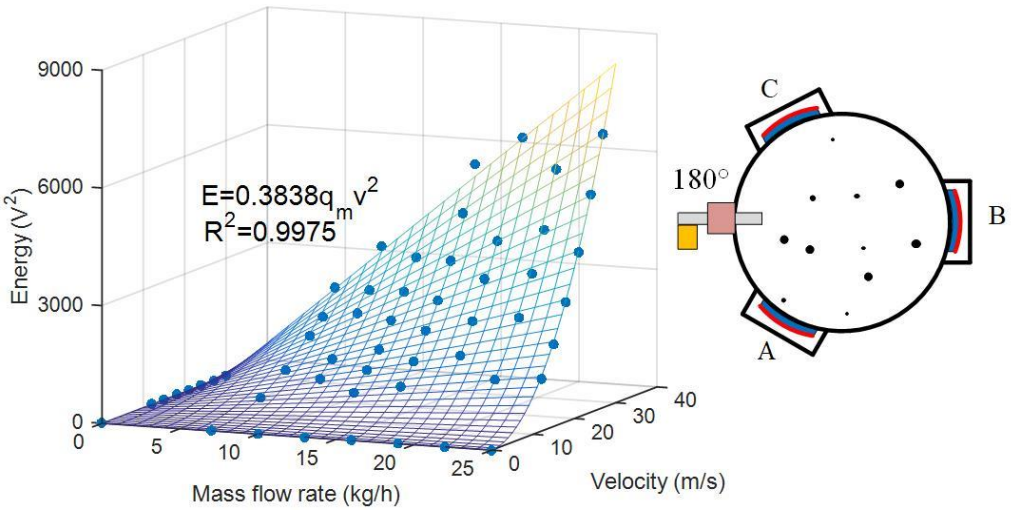

(a)

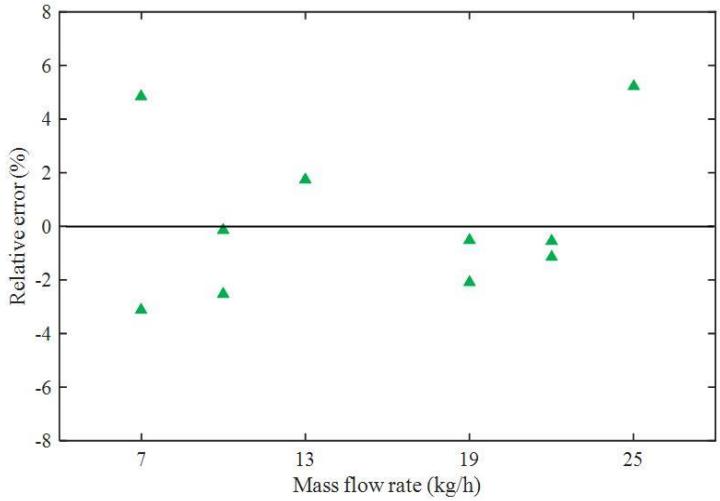

(b)

Fig. 12. Measurement results for the 180° orientation on vertical section of the pipe. (a) AE energy versus the mass flow rate and the particle velocity. (b) Relative error of the measured mass flow rate.

Figs. 13 and 14 illustrate the measurement results from the experiments in which the sensing head was installed in the two orientations (0° and 90°) on the horizontal pipe, respectively. The representing equation and R^2 value are also included in Fig.13 (a). It is evident that the AE energy obtained in the 0° orientation is greater than that in the 90° orientation. This is believed to be due to the fact that more particles are transported at the bottom of the pipe due to the gravitational effect. As can be seen, there is a good agreement between the fitted curves and measured data points with the R^2 values all greater than 0.99. The relative error in the 0° orientation is no greater

than ±5.8%, however this error in the 90° orientation is as high as ±14.7%. This can be explained that, with the sensing head installed in the 90° orientation, the particles impacting the waveguide are poorly representative of the particle flow across the full pipe cross-section. Therefore, for a horizontal pipe, it is best to install the waveguide in the horizontal direction.

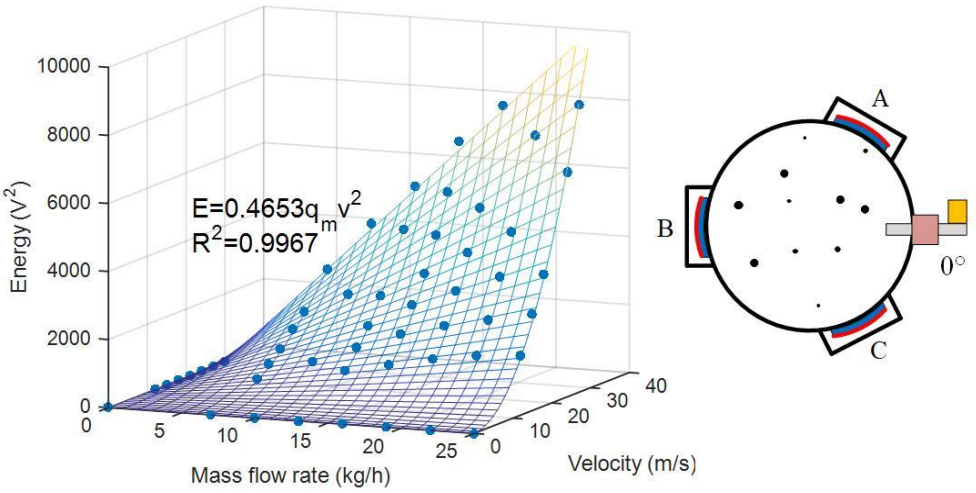

(a)

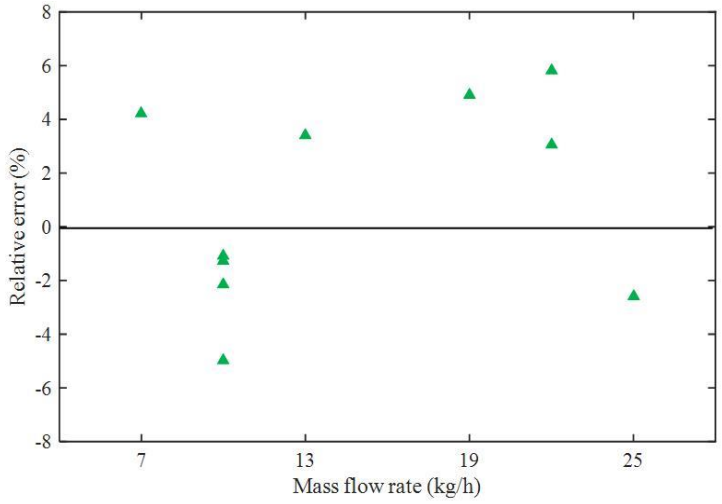

(b)

Fig. 13. Measurement results for the 0° orientation on horizontal section of the pipe. (a) AE energy versus the mass flow rate and the particle velocity. (b) Relative error of the measured mass flow rate.

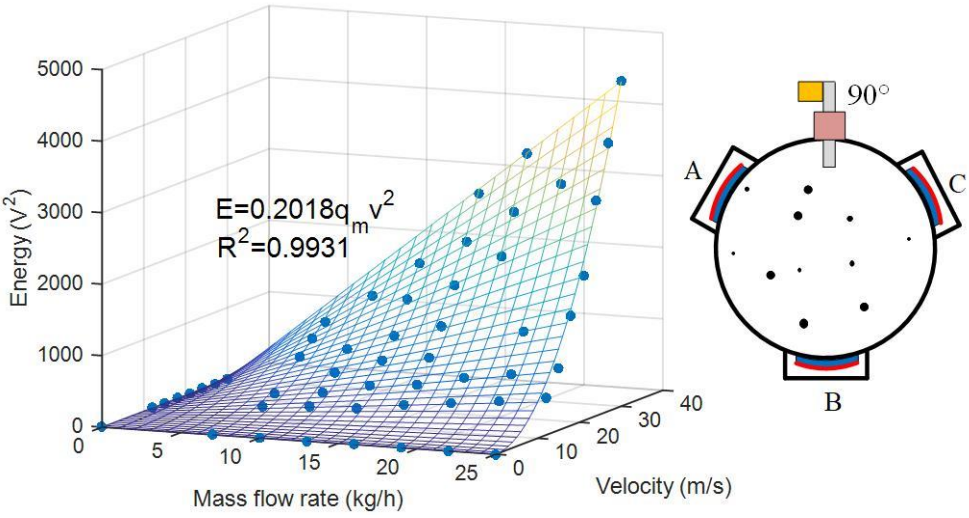

(a)

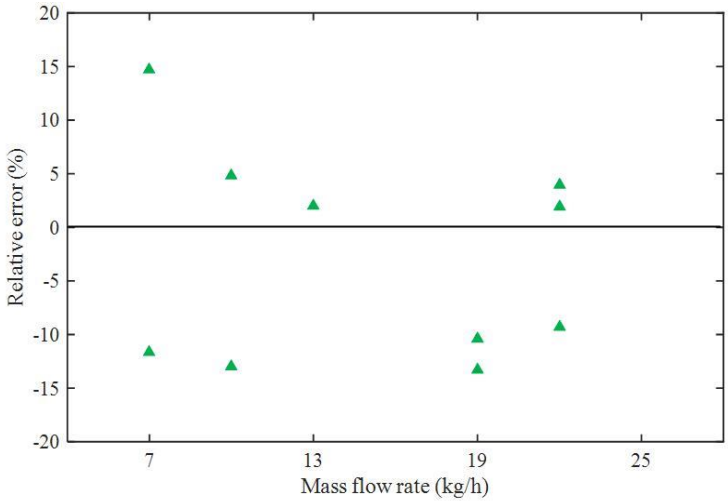

(b)

Fig. 14. Measurement results for the 90° orientation on horizontal section of the pipe. (a) AE energy versus the mass flow rate and the particle velocity. (b) Relative error of the measured mass flow rate.

The solid particles are unevenly distributed across the pipe section while the impact area accounts for a very small proportion of the pipe section. Therefore, the particles that impact the waveguide are not representative of the particle flow across the full pipe cross-section, which is the main factor leading to the error. For a pneumatic conveying pipeline with a large diameter, installing AE sensor devices with different penetration depths in multiple directions around the pipe section will help improve the measurement accuracy.

IV. CONCLUSIONS

This paper has presented a prototype instrumentation system for the online mass flow rate measurement of particles in pneumatic conveying pipelines. A prototype sensing head with an AE probe and three sets of electrostatic sensor arrays each with three arc-shaped electrodes was constructed and evaluated. Meanwhile, an analytical model based on the AE energy has been established. It should be stressed that the meter factor in the analytical model should be calibrated with the target particles to be measured under appropriate ranges of mass flow rate and velocity of particles.

In order to validate the developed instrumentation system, a series of experiments with silica sands as test particles were conducted on both vertical and horizontal pipe sections on the 72-mm bore particle flow test rig. The results have indicated that the relationship among the AE energy, particle velocity and mass flow rate of particles described in the analytical model is consistent with the experimental results. The mass flow rate of particles can therefore be inferred from the AE energy and the particle velocity measured from the electrostatic sensor arrays. The results have also demonstrated that, with the sensing head installed on the vertical section of the pipe, the relative error of the mass flow rate measurement is no greater than ±6.5% over the mass flow rate from 7 kg/h to 25 kg/h and the particle velocity from 12 m/s to 30 m/s regardless of the orientation of the sensing head. This means the sensing head can be installed in any orientation on the vertical section of a pipe. On the horizontal pipe, the waveguide should be in the horizontal direction in order to avoid potential blockage of the pipeline and to obtain representative results. With the waveguide in the horizontal direction when the sensing head is installed on a horizontal pipeline, the relative error in the mass flow metering is within ±5.8% under all test conditions. It is envisaged that the prototype instrumentation system will be trialed, in the near future, on a full-scale coal-

fired power plant or other suitable pneumatic conveying processes where the developed analytical model will be validated and deployed.

ACKNOWLEDGMENT

This work was supported by the National Natural Science Foundation of China under Grant 61573140.

References

[1] T. Deng, J. Li, A. R. Chaudhry, M. Parel, I. Hutchings and M. Bradley, "Comparison between weight loss of bends in a pneumatic conveyor and erosion rate obtained in a centrifugal erosion tester for the same materials," *Wear*, vol. 258, pp. 402–411, 2005.

[2] Y. Zheng and Q. Liu, "Review of certain key issues in indirect measurements of the mass flow rate of solids in pneumatic conveying pipelines," *Measurement*, vol. 43, pp. 727–734, 2010.

[3] Y. Zheng and Q. Liu, "Review of techniques for the mass flow rate measurement of pneumatically conveyed solids," *Measurement*, vol. 44, no. 4, pp. 589–604, 2011.

[4] Y. Lu, D. H. Glass and W. J. Easson, "An investigation of particle behavior in gas–solid horizontal pipe flow by an extended LDA technique," *Fuel*, vol. 88, no. 12, pp. 2520–2531, 2009.

[5] A. Magnussona, R. Rundqvista, A.E. Almstedta and F. Johnssonb, "Dual fibre optical probe measurements of solids volume fraction in a circulating fluidized bed," *Powder Technol.*, vol. 151, pp. 19–26, 2005.

[6] J. Lei, Q. Liu, X. Wang, and S. Liu, "Combination regularization reconstruction method for electrical capacitance tomography," *Flow Meas. Instrum.*, vol. 59, pp. 135–146, 2018.

[7] M. Sun, S. Liu, J. Lei and Z. Li, "Mass flow measurement of pneumatically conveyed solids using electrical capacitance tomography," *Meas. Sci. Technol.*, vol. 19, no. 4, pp. 1–6, 2008.

[8] A. Penirschke and R. Jakoby, "Microwave mass flow detector for particulate solids based on spatial filtering velocimetry," *IEEE Trans. Microw. Theory Tech.*, vol. 56, no. 12, pp. 3193–3199, 2008.

[9] A. Penirschke, M. Puentes, H. Maune, M. Schussler, A. Gaebler and R. Jakoby, "Microwave mass flow meter for pneumatic conveyed particulate solids," in *IEEE Instrumentation and Measurement Technology Conference*, Singapore, 2009.

[10] A. Krein, R. Schenkluhn, A. Kurtenbach, R. Bierl, and J. Barrière, "Listen to the sound of moving sediment in a small gravel-bed river," *Int. J. Sediment Res.*, vol. 31, no. 3, pp. 271–278, 2016.

[11] D. Rickenmann, and B. W. McArdell, "Continuous measurement of sediment transport in the Erlenbach stream using piezoelectric bedload impact sensors," *Earth Surf. Proc. Land.*, vol. 32, no. 9, pp. 1362–1378, 2007.

[12] R. Hou, A. Hunt, and R. A. Williams, "Acoustic monitoring of hydrocyclones," *Powder Technol.*, vol. 124, no. 3, pp. 176–187, 2002.

[13] N. C. Hii, C. K. Tan, S. J. Wilcox, and Z. S. Chong. "An investigation of the generation of acoustic emission from the flow of particulate solids in pipelines," *Powder Technol.*, vol. 243, pp. 120–129, 2013.

[14] Y. Hu, Y. Yan, X. Qian, and W. Zhang, "A comparative study of induced and transferred charges for mass flow rate measurement of pneumatically conveyed particles," *Powder Technol.*, vol.356, pp. 715–725, 2019.

[15] X. Qian, X. Huang, Y. Hu and Y. Yan, "Pulverized coal flow metering on a full-scale power plant using electrostatic sensor arrays," *Flow Meas. Instrum.*, vol. 40, pp. 185–191, 2014.

[16] X. Qian, Y. Yan, X. Huang and Y. Hu, "Measurement of the mass flow and velocity distributions of pulverized fuel in primary air pipes using electrostatic sensing techniques", *IEEE Trans. Meas. Instrum.*, vol. 66, no. 5, pp. 944–952, 2017.

[17] J. Krabicka J and Y. Yan, "Finite-element modeling of electrostatic sensors for the flow measurement of particles in pneumatic pipelines", *IEEE Trans. Meas. Instrum.*, vol. 58, no. 8, pp. 2730–2736, 2009.

[18] J. G. Bouchard, P. A.Payne, and S. Szyszko, “Non-invasive measurement of process states using acoustic emission techniques coupled with advanced signal processing,” *Transactions of the Institution of Chemical Engineers,* vol. 72, pp. 20–25, 1994.

[19] V. Ivantsiv, J. K. Spelt, M. Papini, “Mass flow rate measurement in abrasive jets using acoustic emission,” *Meas. Sci. Technol.,* vol. 20, Art. no. 095402, 2009.

[20] M. G. Droubi, R. L. Reuben and G. White, “Monitoring acoustic emission (AE) energy in slurry impingement using a new model for particle impact,”. *Mech. Syst. Signal Proc.,* vol. 62–63, pp. 415–430, 2015.

[21] K. Wang, Z. Liu, G. Liu, L. Yi, K. Yang, R. Li, M. Chen, and S. Peng, “Vibration sensor approaches for the sand detection in gas–sand two phases flow,” *Powder Technol.,* vol. 288, pp. 221–227, 2016.

[22] G. Zheng, Y. Yan, Y. Hu, W. Zhang, L. Yang and L. Li, “Mass flow rate measurement of pneumatically conveyed particles through acoustic emission detection and electrostatic sensing,” in *IEEE International Instrumentation and Measurement Technology Conference*, Dubrovnik, Croatia, May 25–28, 2020.

[23] M. Arrington, “The use of acoustic emission instrumentation to monitor powder flow,” *NDT International,* vol. 14, pp. 3–8, 1981.

[24] S. C. Hunter, “Energy absorbed by elastic waves during impact,” *J. Mech. Phys. Solids*, vol. 5, pp. 162–171, 1957.

[25] D. J. Buttle, S. R. Martin, and C. B. Scruby, “Particle sizing by quantitative acoustic emission,” *Res. Nondestruct. Eval.*, vol. 3, no. 1, pp. 1–26, 1991.

[26] W. P. Leung, “Demonstration of shear waves, Lamb waves, and Rayleigh waves by mode conversion,” *Am. J. Phys.*, vol. 46, no. 8, pp. 639–642, 1980.

[27] C. Wu, L. Li, and C. Thornton, “Rebound behavior of spheres for plastic impacts,” *Int. J. Impact Eng.*, vol. 28, no. 9, pp. 929–946, 2003.

[28] C. Ruiz-Carcel, A. Starr, and E. Nsugbe, “Estimation of powder mass flow rate in a screw feeder using acoustic emissions,” *Powder Technol.*, vol. 336, 2017.

[29] L. He, Y. Yang, Z. Huang, Z. Liao, J. Wang, and Y. Yang, “Multi-scale analysis of acoustic emission signals in dense-phase pneumatic conveying of pulverized coal at high pressure,” *AIChE J.*, vol. 62, no. 8, pp. 2635–2648, 2016.

[30] Y. Hu, X. Qian, X. Huang, L. Gao and Y. Yan, “On-line continuous measurement of the size distribution of pneumatically conveyed particles by acoustic emission methods,” *Flow Meas. Instrum.*, vol. 40, pp. 163–168, 2014.

[31] C. Xu, J. Li, H. Gao and S. Wang, “Investigations into sensing characteristics of electrostatic sensor arrays through computational modelling and practical experimentation,” *J. Electrost.*, vol. 70, pp. 60–71, 2012.